Free Radical Biology & Medicine 51 (2011) 1996–2006

Contents lists available at SciVerse ScienceDirect

Free Radical Biology & Medicine

journal homepage: www.elsevier.com/locate/freeradbiomed

Original Contribution

Aldosterone increases kidney tubule cell oxidants through calcium-mediated activation of NADPH oxidase and nitric oxide synthase

Nina Queisser [a], Nicole Schupp [a], Helga Stopper [a], Reinhard Schinzel [b], Patricia I. Oteiza [c,*]

[a] Department of Toxicology, University of Würzburg, Würzburg, Germany
[b] Vasopharm GmbH, Würzburg, Germany
[c] Department of Nutrition and Department of Environmental Toxicology, University of California at Davis, Davis, CA 95616, USA

ARTICLE INFO

Article history:
Received 5 May 2011
Revised 22 August 2011
Accepted 25 August 2011
Available online 1 September 2011

Keywords:
Aldosterone
Calcium
Kidney
Free radicals
NADPH oxidase
Nitric oxide synthase
DNA damage

ABSTRACT

Chronic hyperaldosteronism has been associated with an increased cancer risk. We recently showed that aldosterone causes an increase in cell oxidants, DNA damage, and NF-κB activation. This study investigated the mechanisms underlying aldosterone-induced increase in cell oxidants in kidney tubule cells. Aldosterone caused an increase in both reactive oxygen and reactive nitrogen (RNS) species. The involvement of the activation of NADPH oxidase in the increase in cellular oxidants was demonstrated by the inhibitory action of the NADPH oxidase inhibitors DPI, apocynin, and VAS2870 and by the migration of the p47 subunit to the membrane. NADPH oxidase activation occurred as a consequence of an increase in cellular calcium levels and was mediated by protein kinase C. The prevention of RNS increase by BAPTA-AM, W-7, and L-NAME indicates a calcium–calmodulin activation of NOS. A similar pattern of effects of the NADPH oxidase and NOS inhibitors was observed for aldosterone-induced DNA damage and NF-κB activation, both central to the pathogenesis of chronic aldosteronism. In summary, this paper demonstrates that aldosterone, via the mineralocorticoid receptor, causes an increase in kidney cell oxidants, DNA damage, and NF-κB activation through a calcium-mediated activation of NADPH oxidase and NOS. Therapies targeting calcium, NOS, and NADPH oxidase could prevent the adverse effects of hyperaldosteronism on kidney function as well as its potential oncogenic action.

Epidemiological studies have observed an increased cancer incidence in hypertensive individuals [1,2]. A meta-analysis of 10 longitudinal studies, involving approximately 50,000 hypertensive patients, found a 23% higher cancer mortality [3]. In particular, this population showed an increased risk (75% higher for all and 85% higher for women) for developing renal cell carcinoma [1,3,4]. Hyperaldosteronism, contrary to former understanding, is a frequent cause of arterial hypertension, with a prevalence of 8–13% [5–7]. Hyperaldosteronism is also common among patients with resistant hypertension, with a prevalence of 20% [8].

The steroid hormone aldosterone is produced in the adrenal zona glomerulosa upon stimulation by angiotensin II, potassium, or the adrenocorticotropic hormone. Aldosterone regulates blood pressure by maintaining the electrolyte and water homeostasis. This action is exerted through mineralocorticoid receptor-dependent genomic effects in the distal nephron of the kidney [9]. The active aldosterone–receptor complex is translocated into the nucleus, where it binds to hormone-responsive elements in the promoters of target genes, regulating their expression [10]. In addition, aldosterone modulates a rapid, nongenomic signaling pathway. This is most probably mediated also by the classical intracellular mineralocorticoid receptor, but utilizing second messengers [11,12]. Via this rapid signaling, aldosterone causes an increase in the intracellular calcium concentration and is associated with stimulation of phospholipase C, liberation of inositol triphosphate and diacyl glycerol, activation of protein kinase C (PKC)[1], and sodium–proton exchange in the kidney [13,14].

An increase in cell oxidant production and a rapid NADPH oxidase activation by aldosterone were previously described in myocytes [15]. We recently found that aldosterone-induced increase in cellular superoxide anion ($O_2^{\bullet-}$) leads to DNA damage and NF-κB activation [16]. Thus, understanding the mechanisms underlying the pro-oxidant actions of aldosterone could provide insight in the development of new strategies for the prevention of aldosterone-induced kidney

Abbreviations: BAPTA-AM, 1,2-bis(2-aminophenoxy)ethane-*N,N,N′,N′*-tetraacetic acid tetrakis(acetoxymethyl) ester; DAF-FM, 4-amino-5-methylamino-2′,7′-difluorescein; DCF, 5-(and-6)-carboxy-2′,7′-dichlorofluorescein; DHE, dihydroethidium; DPI, diphenyleneiodonium; DTT, dithiothreitol; DMEM, Dulbecco's modified Eagle medium; EDTA, ethylenediamine tetraacetate; EMSA, electrophoretic mobility-shift assay; FBS, fetal bovine serum; Fura-2-AM, Fura-2 pentakis(acetoxymethyl) ester; H_2DCF-DA, 5-(or-6)-carboxy-2′,7′-dichlorodihydrofluorescein diacetate; Hepes, 4-(2-hydroxyethyl)-1-piperazineethanesulfonic acid; L-NAME, L-ne methyl ester; PBS, phosphate-buffered saline; PI, propidium iodide; PKC, protein kinase C; Ro, Ro-32-0432; VAS2870, 3-benzyl-7-(2-benzoxazolyl)thio-1,2,3-triazolo[4,5-d]pyrimidine; W-7, *N*-(6-aminohexyl)-5-chloro-1-naphthalenesulfonamide hydrochloride.

* Corresponding author. Fax: +530 752 8966.
E-mail address: poteiza@ucdavis.edu (P.I. Oteiza).

0891-5849/$ – see front matter © 2011 Elsevier Inc. All rights reserved.
doi:10.1016/j.freeradbiomed.2011.08.028

damage. One of the main sources of $O_2^{\bullet-}$ production in cells is the enzyme NADPH oxidase. Initially described in the hematopoietic system, NADPH oxidase was subsequently found in different cell types where it can play an important role in cell signaling modulation. The activation of NADPH oxidase requires the recruitment of the main membrane integral subunit NOX with other membrane (p22phox) and cytosolic (p47phox, p67phox, p40phox, and Rac) components. The NOX components exist in various isoforms and have a distinct cellular localization in the kidney. NOX2 and NOX4 are present in a cell line model of renal proximal tubule cells (human hRPT) [17] and NOX1 and NOX4 are prominently expressed in the distal tubules [18]. The binding of various ligands to receptors that trigger the activation of signaling cascades is often associated with NADPH oxidase activation. In the kidney, NADPH oxidase can participate in the maintenance of ion homeostasis, regulating tubular sodium and potassium transport [19]. Although NADPH oxidase activation and the consequent production of reactive oxygen species (ROS) have important physiological functions, a chronic aldosterone-induced NADPH oxidase activation could lead to cellular damage and transformation.

Although the exact mechanisms of NADPH oxidase activation are not fully described, it is known that calcium is a critical NADPH oxidase regulator, activating the enzyme either directly or indirectly. Calcium, via calmodulin, also activates nitric oxide synthase (NOS), an enzyme that catalyzes the synthesis of nitric oxide (NO) via a five-electron oxidation of a guanidine group in L-arginine [20]. NO is a very important molecule in cell signaling, regulating important physiological processes. On the other hand, NO can chemically modify proteins, and its reaction with $O_2^{\bullet-}$ generates the highly reactive species peroxynitrite [21]. The interplay between NADPH oxidase, calcium, and NOS is considered very relevant in redox signaling [22].

Recent evidence showing that the calcium channel blocker dihydropyridine protects the kidney from aldosterone-induced NADPH oxidase activation and injury in rats [23] strongly suggests a role for calcium in aldosterone-induced oxidant increase in kidney cells. Thus, this work investigated the involvement of calcium in aldosterone-induced NADPH oxidase activation and increased ROS production in kidney tubule cells. The potential capacity of aldosterone to cause NOS activation and an increase in cellular reactive nitrogen species (RNS) was also investigated. The roles of calcium-mediated NADPH oxidase and NOS activation by high aldosterone on DNA oxidative damage and NF-κB activation were investigated as two major functional consequences of hyperaldosteronism in kidney cells [16].

Materials and methods

Materials

MDCK and LLC-PK1 cells were obtained from the American Type Culture Collection (Manassas, VA, USA). Cell culture media and reagents were obtained from PAA Laboratories GmbH (Pasching, Austria) and Invitrogen Life Technologies (Carlsbad, CA, USA), respectively. The primary antibody against p47phox (sc-14015) was obtained from Santa Cruz Biotechnology (Santa Cruz, CA, USA) and α-tubulin (T6199) was purchased from Sigma (St. Louis, MO, USA). The oligonucleotide containing the consensus sequence for NF-κB and SP-1 and the reagents for the electrophoretic mobility-shift assay (EMSA) were obtained from Promega (Madison, WI, USA). Polyvinylidene difluoride (PVDF) membranes were obtained from Bio-Rad (Hercules, CA, USA) and Chroma Spin-10 columns from Clontech (Palo Alto, CA, USA). The ECL Plus Western blotting system was from Amersham Pharmacia Biotech (Piscataway, NJ, USA). Fura-2 pentakis(acetoxymethyl) ester (Fura-2-AM), 5-(and-6)-carboxy-2′,7′-dichlorodihydrofluorescein diacetate (H_2DCF-DA), and propidium iodide (PI) were obtained from Molecular Probes (Eugene, OR, USA). Apocynin was obtained from Calbiochem (San Diego, CA, USA). Aldosterone, 1,2-bis(2-aminophenoxy)ethane-*N,N,N′,N′*-tetraacetic acid tetrakis(acetoxymethyl) ester (BAPTA-AM), 4-amino-5-methylamino-2′,7′-difluorescein (DAF-FM), diphenyleneiodonium chloride (DPI), eplerenone, L-nitroarginine methyl ester (L-NAME), *N*-(6-aminohexyl)-5-chlor-1-naphthalinsulfonamid (W-7), mifepristone, Ro-32-0432 (Ro), Tempol, and all other reagents were of the highest quality available and were purchased from Sigma. VAS2870 was kindly donated by vasopharm GmbH (Würzburg, Germany). DHE was obtained from Merck Biosciences GmbH (Schwalbach, Germany).

Cell culture

LLC-PK1 cells were cultured at 37 °C, 5% CO_2 in DMEM low glucose (1 g/L) supplemented with 10% (v/v) fetal bovine serum (FBS), 1% (w/v) L-glutamine, 2.5% (w/v) Hepes, and antibiotics (50 U/ml penicillin, 50 μg/ml streptomycin). MDCK cells were cultured at 37 °C, 5% CO_2 in minimum essential medium with Earle's salts supplemented with 10% (v/v) FBS, 1% (w/v) L-glutamine, and antibiotics (50 U/ml penicillin, 50 μg/ml streptomycin). At confluence, LLC-PK1 and MDCK cell medium was replaced, and 24 h later cells were treated with 10 or 100 nM aldosterone. The incubation times and the presence of various inhibitors are described for each experiment.

Evaluation of the concentration of intracellular oxidants

The concentration of intracellular oxidants was estimated using the probe H_2DCF-DA. Cells (1.5×10^4) were seeded in 96-well plates, and at confluence, were incubated without or with the addition of 100 nM aldosterone for 30 (LLC-PK1) or 120 (MDCK) min. After 20 (LLC-PK1) or 90 (MDCK) min of incubation with aldosterone, 40 μM H_2DCF-DA was added, and cells were further incubated for 10 (LLC-PK1) or 30 (MDCK) min. The medium was removed, cells were rinsed with phosphate-buffered saline (PBS), and 200 μl of PBS was added per well. Fluorescence was measured at λ_{ex} 475 nm, λ_{em} 525 nm. To determine the DNA content, samples were subsequently incubated with 0.1% (v/v) Igepal and 50 μM PI and incubated for 20 min at room temperature, and the fluorescence (λ_{ex} 538 nm, λ_{em} 590 nm) was measured. Results are expressed as the ratio of DCF fluorescence/PI fluorescence.

Cell oxidants were also measured using the probe dihydroethidium. Cells (0.2×10^6) were seeded on 12-mm coverslips the day before treatment. At the end of the corresponding incubations, the medium was removed, and the cells were washed twice with PBS. Fresh medium containing 5 μM DHE was added, and the cells were incubated for 30 min at room temperature in the dark. After a wash with PBS, cell fluorescence was measured by confocal fluorescence microscopy with an Eclipse 55i microscope (Nikon GmbH, Düsseldorf, Germany) and a Fluoro Pro MP 5000 camera (Intas Science Imaging Instruments GmbH, Göttingen, Germany) at 200-fold magnification. Quantification was done by measuring gray values of 200 cells per treatment using the routines available in ImageJ 1.40 g (http://rsb.info.nih.gov/ij/) [24].

Evaluation of the concentration of intracellular RNS

The concentration of intracellular nitrogen species was estimated using the probe DAF-FM. Cells (1.5×10^4) were seeded in 96-well plates and incubated with or without 100 nM aldosterone for 30 (LLC-PK1) or 120 (MDCK) min. Cells were subsequently washed in PBS and incubated in cell culture medium containing 10 μM DAF-FM, for 30 min at room temperature in the dark. The medium was subsequently removed, cells were rinsed with PBS, and 200 μl of PBS was added per well. Fluorescence was measured at λ_{ex} 495 nm, λ_{em} 515 nm. To determine the DNA content, samples were subsequently incubated with 0.1% (v/v) Igepal and 50 μM PI and incubated for 20 min at room temperature, and the fluorescence (λ_{ex} 538 nm, λ_{em}

590 nm) was measured. Results are expressed as the ratio of DAF-FM fluorescence/PI fluorescence.

Evaluation of cellular RNS by scanning laser confocal microscopy

Cells (0.2×10^6) were seeded on 12-mm coverslips the day before treatment. Cells were treated with or without 10 nM aldosterone and the NOS inhibitors L-NAME (50 μM) and W-7 (10 μM) for 30 min (LLC-PK1) or 2 h (MDCK). At the end of the treatments, the cells were washed once with PBS and incubated in medium containing 10 μM DAF-FM for 15 min at room temperature in the dark. After a wash with PBS, fluorescence at 515 nm (λ_{ex} 495) was measured using a TCS SP5 laser scanning confocal microscope (Leica Microsystems GmbH, Wetzlar, Germany).

Evaluation of intracellular calcium levels

Cells (0.5×10^4) were seeded in 96-well plates for 24 h. At confluence, they were incubated with or without 10 nM aldosterone or the corresponding substances for 30 (LLC-PK1) or 120 (MDCK) min. The medium was subsequently removed, and the cells were rinsed with PBS and incubated in medium containing 10 μM Fura-2-AM for 30 min at room temperature in the dark. The cells were washed with PBS, and fluorescence was measured at 510 nm (λ_{ex} 340). Results are expressed as the fluorescence emission (λ_{em} 510 nm) at λ_{ex} 340 nm.

Evaluation of intracellular calcium levels by laser scanning confocal microscopy

Cells (7×10^5) were seeded on 12-mm coverslips. At confluence the cells were incubated in medium with or without 10 nM aldosterone and the corresponding substances for 30 (LLC-PK1) or 120 (MDCK) min. At the end of the treatment, the cells were incubated in medium containing 5 μM Fura-2-AM for a further 10 min, at 37 °C in the dark. The medium was subsequently removed, and the cells were washed twice with PBS. Confocal images were obtained by measuring the fluorescence at 510 nm (λ_{ex} 405 nm) using a TCS SP5 laser scanning confocal microscope (Leica Microsystems GmbH).

EMSA

Nuclear fractions were isolated as previously described [25]. For the EMSA, oligonucleotides containing the consensus sequence of NF-κB or SP-1 were end labeled with [γ-^{32}P]ATP using T4 polynucleotide kinase and purified using Chroma Spin-10 columns. Samples were incubated with the labeled oligonucleotide (20,000–30,000 cpm) for 20 min at room temperature in 1× binding buffer [5× binding buffer: 50 mM Tris–HCl buffer, pH 7.5, containing 20% (v/v) glycerol, 5 mM $MgCl_2$, 2.5 mM EDTA, 2.5 mM DTT, 250 mM NaCl, and 0.25 mg/ml poly(dI–dC)]. The products were separated by electrophoresis in a 6% (w/v) nondenaturing polyacrylamide gel using 0.5× TBE (Tris/borate 45 mM, EDTA 1 mM) as the running buffer. The gels were dried and the radioactivity was quantified in a Phosphoimager 840 (Amersham Pharmacia Biotech, Piscataway, NJ, USA).

Western blot analysis

For the preparation of cytosolic fractions, cells (5×10^6) were rinsed with PBS, scraped, and centrifuged at 1000 *g* for 5 min at 4 °C. The cell pellet was rinsed with PBS and resuspended in 80–200 μl of 10 mM Hepes (pH 8) containing 1.5 mM $MgCl_2$, 5 mM KCl, 0.5 mM DTT, 0.5 mM phenylmethylsulfonyl fluoride, 0.4 mM $NaVaO_4$, protease inhibitors, and 0.2% (v/v) Igepal. Samples were incubated at 4 °C for 10 min and centrifuged at 14,000 rpm. The supernatant was transferred into a new tube and the protein concentration was measured [26].

For Western blotting, proteins (50 μg) were separated by SDS–PAGE (12.5%), blotted on PVDF membranes, and incubated overnight at 4 °C with the primary rabbit p47phox antibody (1:500 dilution) and 90 min at room temperature in the presence of the secondary horseradish peroxidase-conjugated antibody. Chemiluminescence detection was done with SuperSignal West Dura extended duration substrate (Thermo Scientific). Band density was quantified using Gel Doc 2000 with the software Multi-Analyst version 1.0.2 (Bio-Rad). As loading control, membranes were stripped and probed for α-tubulin as described above.

Comet assay

The comet assay was done as described before [27]. Briefly, cells were treated for 4 h with the tested substances. Afterward, the cells were embedded in agarose and exposed to an electrical field. From cells with damaged DNA (single- or double-strand breaks, alkali labile sites), more DNA can migrate than from cells with intact nuclear DNA. A comet-like structure is formed because smaller fragments and relaxed loops move faster than larger fragments and intact DNA. DNA was stained with PI (20 μg/ml). A fluorescence microscope at 200-fold magnification, and a computer-aided image analysis system (Komet 5; Kinetic Imaging Ltd, Liverpool, UK), were used for analysis. Fifty cells in total (25 per slide) were analyzed per experimental condition, and results were expressed as percentage of DNA in the tail region.

Determination of formamidopyrimidine DNA glycosylase (FPG)-sensitive sites

FPG-sensitive sites were determined by comet assay, including a previous incubation step with 0.05 μg/ml FPG protein, kindly donated

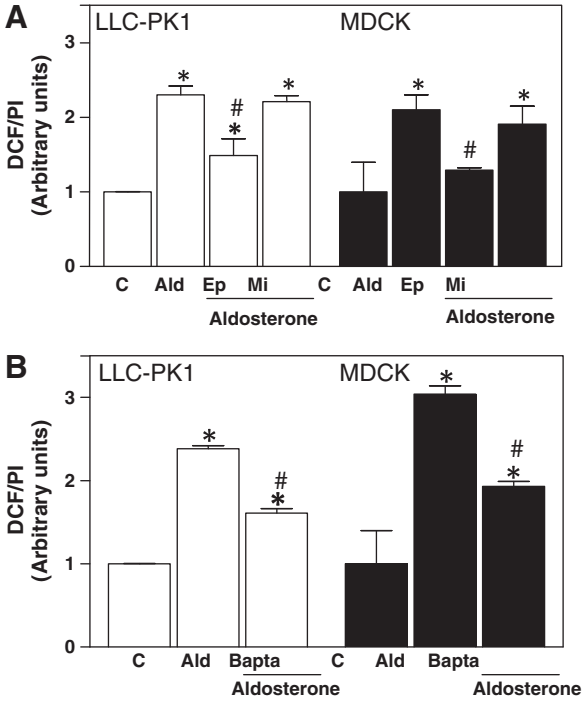

Fig. 1. Aldosterone induces a calcium-mediated increase in LLC-PK1 and MDCK cell oxidant levels. LLC-PK1 and MDCK cells were incubated in the absence (C) and presence of 100 nM aldosterone. Aldosterone-treated cells were simultaneously incubated without (Ald) or (A) with 0.5 μM eplerenone (Ep) or 0.5 μl mifepristone (Mi), aldosterone receptor and glucocorticoid receptor antagonists, respectively, or (B) with the calcium chelator BAPTA-AM (Bapta; 10 μM). Cellular oxidant levels were measured using the probe H_2DCF-DA after incubating LLC-PK1 and MDCK cells for 30 and 120 min, respectively. DCF fluorescence was normalized to PI fluorescence. Results are shown as means ± SEM of at least three independent experiments. $^*p\leq0.05$ vs control, $^\#p\leq0.05$ vs aldosterone treatment.

by Professor Bernd Epe (Institute for Pharmacy, University of Mainz, Germany), as described earlier [28].

Micronucleus frequency test

Micronuclei are expressed in dividing cells that contain chromosome breaks (resulting from unrepaired double-strand breaks) and/or whole chromosomes that are unable to travel to the spindle poles during mitosis. They are observed in cells with completed nuclear division and are scored in the binucleated stage of the cell cycle by using the cytokinesis inhibitor cytochalasin B. The micronucleus frequency test was performed as described earlier [27]. Cells were incubated for 4 h with the tested compounds, then 3 μg/ml cytochalasin B was added for 24 h to obtain binucleated (BN) cells. For each experimental condition, the frequency of micronuclei was obtained after scoring 1000 BN cells on each of two slides at a 500-fold magnification.

Statistics

For comet assay, micronucleus frequency test, and superoxide quantification results, the Mann–Whitney test was used to determine significance between two groups, calculated with SPSS 17.0. For the rest of the assays, one-way analysis of variance with subsequent post hoc comparisons by Scheffe were performed using StatView 5.0 (SAS Institute, Cary, NC, USA). A p value ≤ 0.05 was considered statistically significant. Values are given as means ± SEM and are the average of at least three independent experiments.

Results

Aldosterone induces a calcium-mediated increase in ROS and RNS production via the mineralocorticoid receptor

Two kidney cell lines (LLC-PK1, MDCK) with different functional characteristics were chosen to study the mechanisms involved in the increased oxidant production associated with exposure to high aldosterone levels. LLC-PK1 cells are from pig kidney and resemble proximal tubule cells [29], and MDCK cells are from dog kidney and resemble distal tubule cells [30].

Mineralocorticoid and glucocorticoid receptors are expressed in LLC-PK1 [31] and MDCK cells (data not shown). To investigate if the aldosterone-triggered increase in cellular oxidants is mediated exclusively via the mineralocorticoid receptor, antagonists of the mineralocorticoid (eplerenone) and glucocorticoid (mifepristone) receptors were used. Cell oxidants were evaluated using H_2DCF-DA, a nonfluorescent probe that, once inside cells, can be oxidized to a fluorescent derivative (DCF) by endogenous oxidants (ROS and

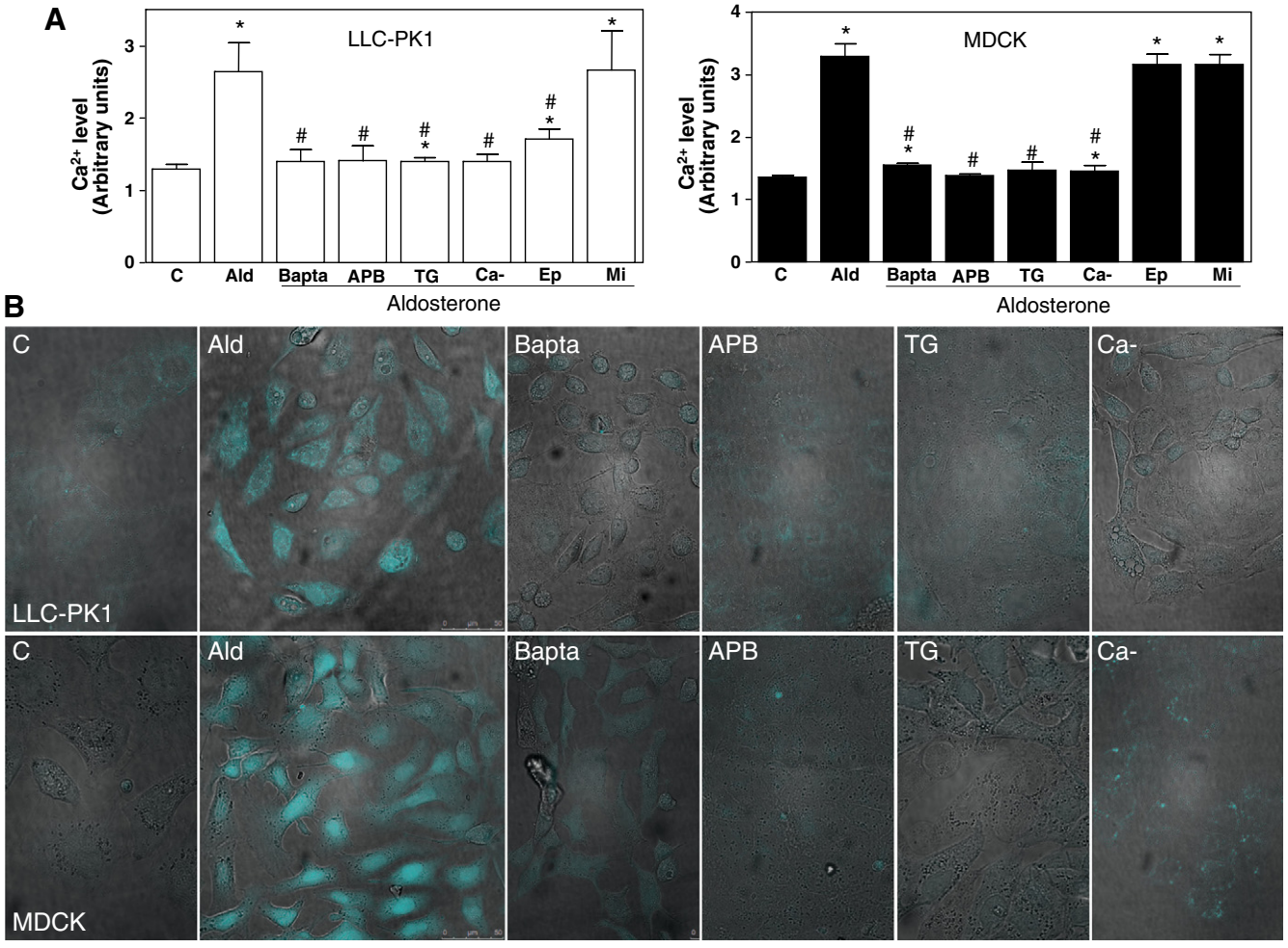

Fig. 2. Aldosterone induces an increase in LLC-PK1 and MDCK cell calcium levels. LLC-PK1 and MDCK cells were incubated in the absence (C) and presence of 10 nM aldosterone. Aldosterone-treated cells were simultaneously incubated without (Ald) or with 10 μM BAPTA-AM (Bapta; calcium chelator), 5 μM 2-APB (APB; inhibitor of store-operated calcium channels and IP_3 receptors), or 0.2 μM thapsigargin (TG; sarcoplasmic/endoplasmic reticulum calcium inhibitor), or in calcium-free medium (Ca−). Cellular calcium levels were evaluated with the probe Fura-2-AM by (A) spectrofluorimetry or (B) confocal microscopy. (A) Fura-2-AM fluorescence (λ_{ex} 340, λ_{em} 510 nm) values are shown as arbitrary units. Results are shown as means ± SEM of three independent experiments. $^{*}p \leq 0.05$ vs control, $^{\#}p \leq 0.05$ vs aldosterone treatment. (B) Confocal microscopy of LLC-PK1 (top) and MDCK cells (bottom). Confocal images were obtained by measuring the fluorescence at 510 nm (λ_{ex} 405 nm).

RNS) [32]. Eplerenone significantly inhibited aldosterone-induced DCF fluorescence increase in both LLC-PK1 and MDCK cells (67 and 86%, respectively), whereas mifepristone had no effect (Fig. 1A). These results indicate that aldosterone increases ROS and RNS mostly via the mineralocorticoid receptor.

NADPH oxidase and NOS are important cellular sources of ROS and RNS. Both enzymes can be activated by a rise in cellular calcium. Thus, the role of calcium in aldosterone-induced increase in cellular oxidant production was next investigated. The cell-permeative intracellular calcium chelator BAPTA-AM caused a 56 and 54% inhibition of the

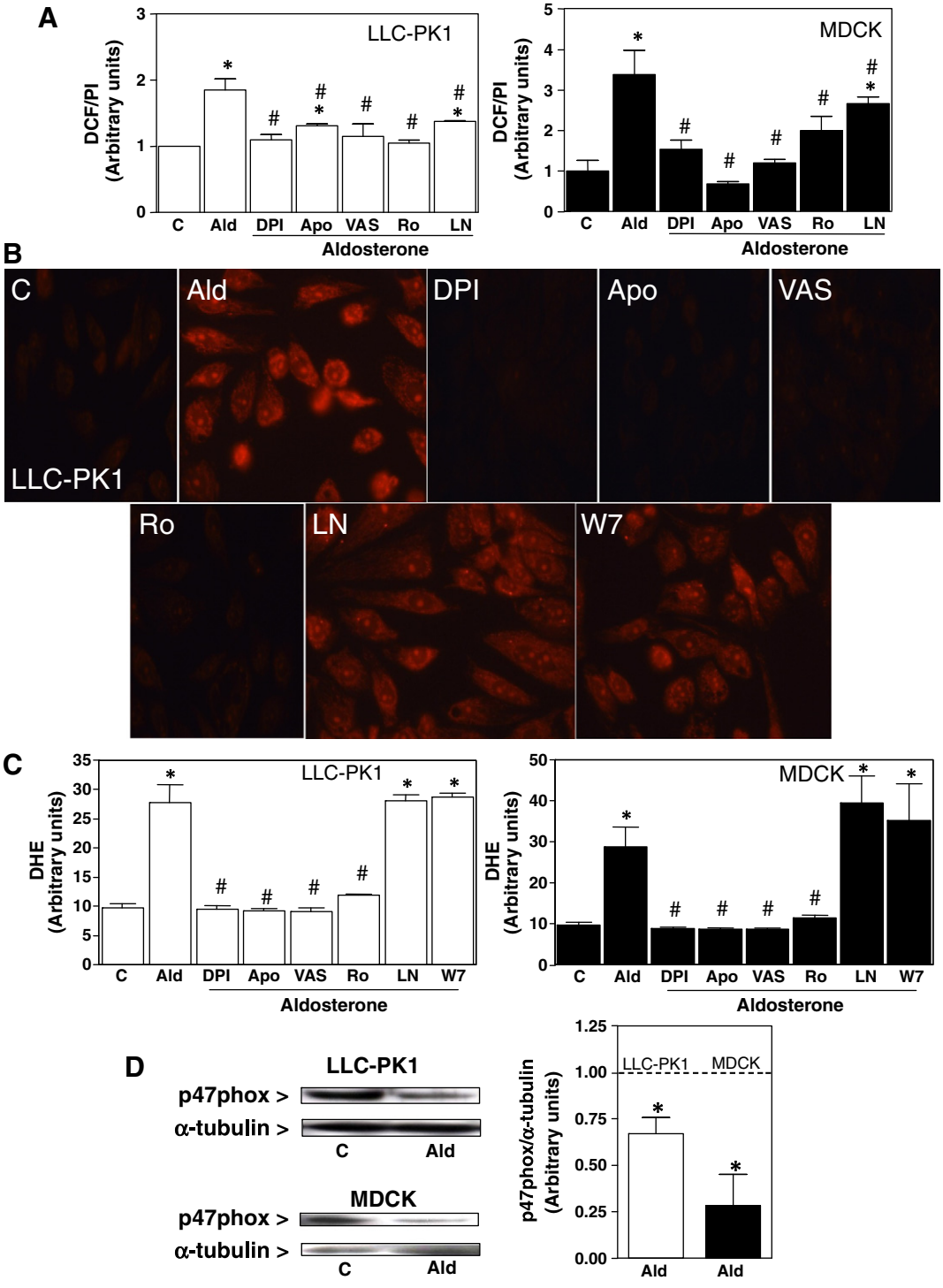

Fig. 3. Aldosterone induces ROS increase in LLC-PK1 and MDCK cells through NADPH oxidase activation. LLC-PK1 and MDCK cells were incubated in the absence (C) and presence of aldosterone for 30 and 120 min, respectively. Aldosterone-treated cells were simultaneously incubated without (Ald) or with 1 μM DPI (DPI), 50 μM apocynin (Apo), 1 μM VAS2870 (VAS) (NADPH oxidase inhibitors); 1 μM Ro (Ro; PKC inhibitor); 50 μM L-NAME (LN; NOS inhibitor); or 10 μM W-7 (W7; calmodulin inhibitor). (A) Cellular oxidant levels were measured with the probe H_2DCF-DA after incubating LLC-PK1 and MDCK cells for 30 and 120 min, respectively, with 100 nM aldosterone. DCF fluorescence was normalized to PI fluorescence. (B, C) Cellular oxidant levels were also evaluated using the probe DHE after incubating the cells with 10 nM aldosterone. (B)Representative confocal microscopy images. (C)Images were quantified and results expressed as arbitrary units. (D) Cytosolic fractions were isolated and p47phox and α-tubulin were detected by Western blot. Left: representative images. Right: bands were quantitated and p47phox content was referred to α-tubulin content as loading control. All results are shown as means ± SEM of at least three independent experiments. $^{*}p \leq 0.05$ vs control, $^{\#}p \leq 0.05$ vs aldosterone treatment.

aldosterone-mediated increase in DCF fluorescence in LLC-PK1 and MDCK cells, respectively (Fig. 1B).

Aldosterone triggers an increase in cellular calcium levels

Based on the above results, the possibility that aldosterone could trigger an increase in cellular calcium was subsequently investigated. Intracellular calcium was measured in LLC-PK1 and MDCK cells using the cell-permeative calcium probe Fura-2-AM, at the time points of maximal oxidant production (30 and 120 min for LLC-PK1 and MDCK cells, respectively). Fura-2-AM fluorescence was significantly higher in LLC-PK1 and MDCK cells treated with 10 nM aldosterone compared to untreated cells (Fig. 2A). Eplerenone, an aldosterone receptor antagonist, inhibited aldosterone-induced Fura-2-AM fluorescence increase in LLC-PK1 cells, but not in MDCK cells, whereas mifepristone, a glucocorticoid receptor antagonist, had no effect in either cell line. These results indicate the involvement of the mineralocorticoid receptor, but not the glucocorticoid receptor, in the aldosterone-induced calcium increase in LLC-PK1 cells. In MDCK cells, the rise in cellular calcium is independent of the binding of aldosterone to both receptors. Aldosterone-induced cellular calcium increase was prevented by 2-APB, an inhibitor of store-operated calcium channels [33] and inositol triphosphate (IP_3) receptors [34] (Fig. 2), suggesting that aldosterone promotes the mobilization of calcium through these structures. Aldosterone-induced increase in cellular Fura-2-AM fluorescence was prevented by the calcium chelator BAPTA-AM and by the sarcoplasmic/endoplasmic reticulum calcium inhibitor thapsigargin and when cells were incubated in calcium-free medium (Fig. 2).

Aldosterone causes an increase in cellular ROS through NADPH oxidase activation

Previous evidence from our group showed that aldosterone causes an increase in $O_2^{\bullet-}$ levels in kidney cells [16]. NADPH oxidase is a major source of $O_2^{\bullet-}$ in cells and can be activated by calcium. To investigate the potential involvement of this enzyme in the increased cell oxidant levels associated with high aldosterone levels, we investigated the effects of the NADPH oxidase inhibitors DPI, apocynin, and VAS2870. DPI is widely used to inhibit NADPH oxidase but is not specific, given that it also inhibits other enzymes requiring reduction of the cofactor flavin adenine dinucleotide. In contrast, apocynin selectively blocks the translocation of the cytosolic NADPH oxidase components to the membrane, which is required for NADPH oxidase activation. However, apocynin is currently suspected to have per se antioxidant capacity [35]. VAS2870 has been identified as a NADPH oxidase inhibitor by specific high-throughput screening, although its exact mechanism of action is still unknown [36]. All three NADPH oxidase inhibitors completely inhibited the aldosterone-mediated increase in DCF fluorescence in LLC-PK1 and MDCK cells (Fig. 3A). The inhibition of DCF increase by the PKC inhibitor Ro indicates that NADPH oxidase activation occurs, at least in part, through the activation of PKC by aldosterone-induced cellular calcium increase. The partial prevention of DCF fluorescence increase when cells were simultaneously

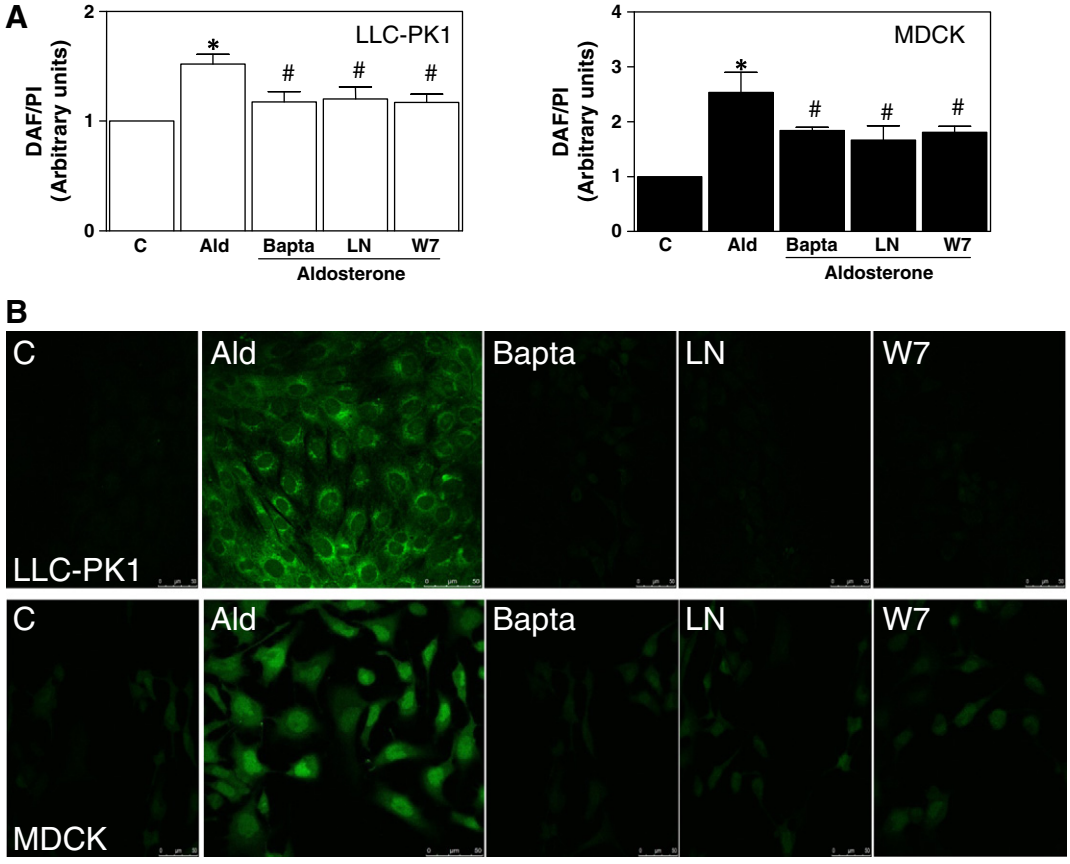

Fig. 4. Aldosterone induces a calcium-mediated increase in LLC-PK1 and MDCK cell RNS levels. LLC-PK1 and MDCK cells were incubated in the absence (C) and presence of aldosterone (Ald). Aldosterone-treated cells were simultaneously incubated with 10 μM BAPTA-AM (Bapta; calcium chelator), 50 μM L-NAME (LN; NOS inhibitor), and 10 μM W-7 (W7; calmodulin inhibitor). DAF-FM fluorescence was measured (A) after incubating the cells with 100 nM aldosterone by spectrofluorimetry or (B) after incubating the cells with 10 nM aldosterone by confocal microscopy. (A) DAF-FM fluorescence was normalized to PI fluorescence. Results are shown as means ± SEM of at least three independent experiments. $^{*}p \leq 0.05$ vs control, $^{\#}p \leq 0.05$ vs aldosterone treatment. (B) Confocal microscopy of LLC-PK-1 cells (top) and MDCK cells (bottom).

incubated with aldosterone and the NOS inhibitor L-NAME suggests that cellular RNS production is regulated by aldosterone (Fig. 3A). However, it should be taken into consideration that L-NAME could inhibit the NOS-mediated generation of $O_2^{\bullet-}$ if NOS is uncoupled by aldosterone [37]. Nevertheless, the involvement of RNS in the actions of aldosterone is additionally supported by the results obtained with the NO-sensitive probe DAF.

To further strengthen the hypothesis that aldosterone-mediated production of ROS is mediated via NADPH oxidase, the increased oxidant cell levels and the potential inhibition by NADPH oxidase inhibitors were next investigated using the probe DHE, which is converted to a fluorescent derivative mainly by reaction with $O_2^{\bullet-}$. Fig. 3B shows representative images of the effects of aldosterone, and of the various inhibitors, on DHE fluorescence in LLC-PK1 cells. DHE fluorescence was 2.6- and 2.9-fold higher after 30 and 120 min incubation with 10 nM aldosterone in LLC-PK1 cells and MDCK cells, respectively (Fig. 3C). As also observed with DCF, this increase was prevented by the simultaneous incubation of cells with the NADPH oxidase inhibitors DPI, apocynin, and VAS2870 and with the PKC inhibitor Ro. In contrast, the NOS inhibitor L-NAME and the calmodulin inhibitor W-7 did not affect aldosterone-induced increase in DHE fluorescence.

To confirm NADPH oxidase activation, we subsequently measured the translocation of the cytosolic subunit p47phox to the cell membrane, an event that is required for the activation of NADPH oxidase. p47phox levels in cytosolic fractions, as measured by Western blot, were significantly lower in LLC-PK1 and MDCK cells incubated with aldosterone for 30 and 120 min, respectively (Fig. 3C).

Aldosterone causes an increase in cellular RNS through NOS activation

Given that the probe H_2DCF-DA can react with both ROS and RNS, and that NOS can also be activated by calcium, we next investigated if aldosterone could also increase RNS production. For this purpose, we used DAF-FM, which is a sensitive probe for the detection of NO. Aldosterone caused a 51 and 154% increase in DAF-FM fluorescence in LLC-PK1 and MDCK cells, respectively, which was significantly inhibited by the calcium chelator BAPTA-AM as demonstrated by biochemical quantification (Fig. 4A) and confocal microscopy (Fig. 4B).

The prevention of the increase in DAF-FM fluorescence by the NOS inhibitor L-NAME indicates that aldosterone activates NOS with a consequent increase in NO synthesis. The inhibitory action of the calcium chelator BAPTA-AM and of the calmodulin inhibitor W-7 indicates that aldosterone-induced activation of NOS occurs via calcium–calmodulin (Figs. 4A and B).

NADPH oxidase and NOS activation are involved in aldosterone-induced NF-κB activation

The activation of NF-κB, measured as NF-κB–DNA binding in nuclear fractions by EMSA, was next investigated as a potential functional consequence of NADPH oxidase and NOS activation. The involvement of ROS and of aldosterone-mediated activation of NADPH oxidase via PKC was evidenced by the inhibition of the increase in NF-κB–DNA binding by the NADPH oxidase inhibitors

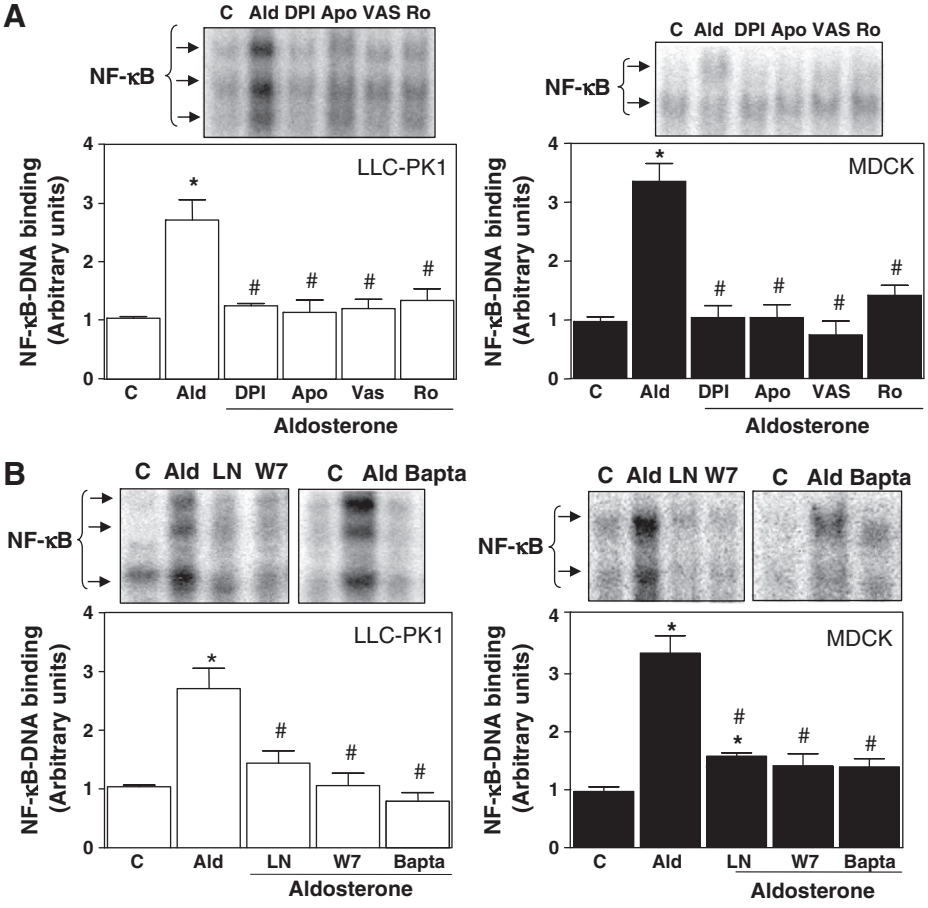

Fig. 5. Aldosterone activates NF-κB in LLC-PK1 and MDCK cells through calcium-mediated NOX and NOS activation. NF-κB–DNA binding was measured by EMSA in nuclear fractions from LLC-PK1 and MDCK cells, incubated in the absence (C) and presence of 100 nM aldosterone for 30 and 120 min, respectively. Aldosterone-treated cells were simultaneously incubated without (Ald) or with (A) 1 μM DPI (DPI), 50 μM apocynin (Apo), or 1 μM VAS2870 (VAS) (NADP oxidase inhibitors) or 1 μM Ro (Ro; PKC inhibitor) or with (B) 50 μM L-NAME (LN; NOS inhibitor), 10 μM W-7 (W7; calmodulin inhibitor), or the calcium chelator BAPTA-AM (Bapta; 10 μM). The intensity of the bands corresponding to the NF-κB–DNA complexes was measured. Results are shown as means ± SEM of at least five independent experiments. $^{*}p \leq 0.05$, significantly different from the control, and $^{\#}p \leq 0.05$, significantly different from the aldosterone-treated group.

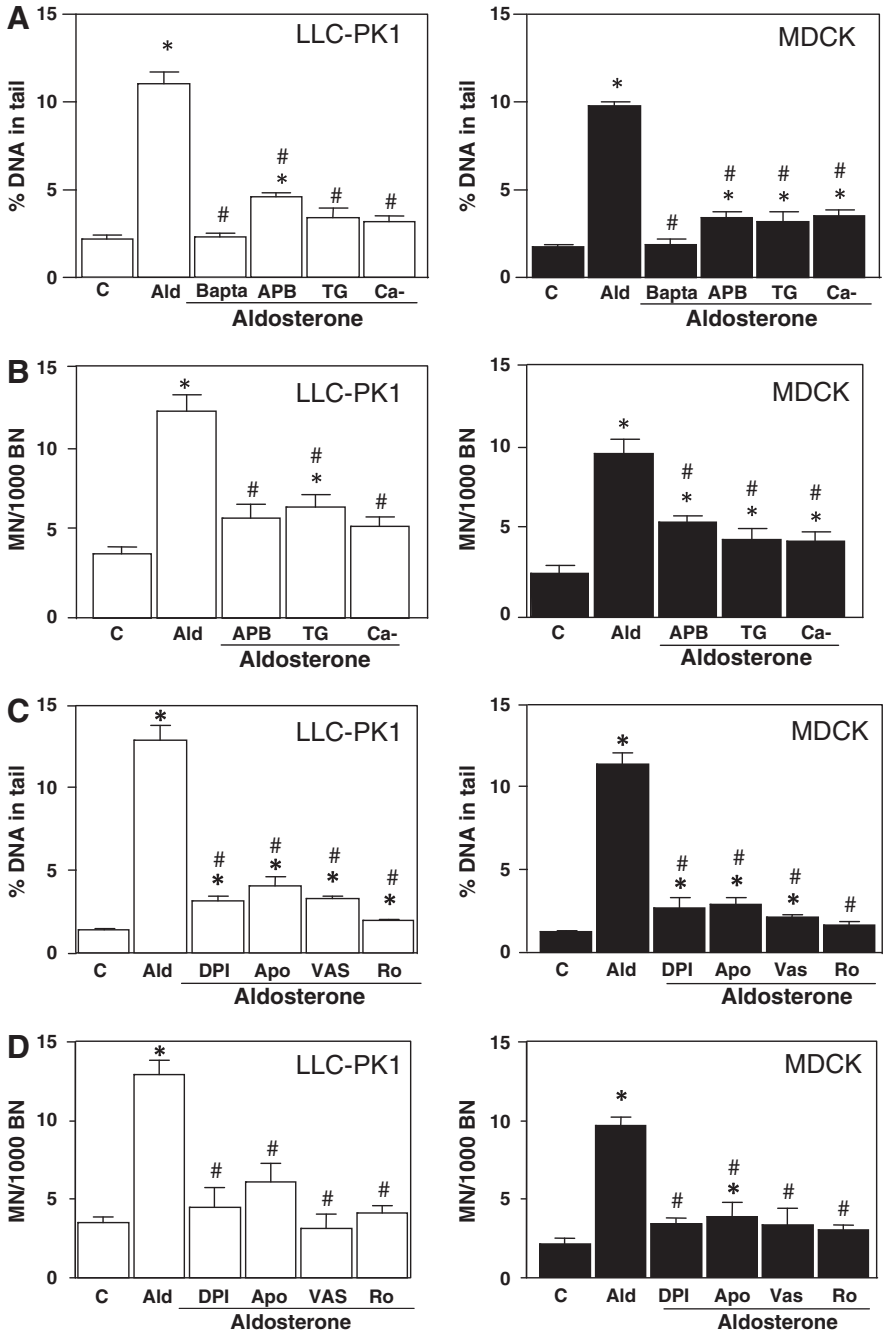

Fig. 6. Aldosterone induces DNA damage via calcium-mediated activation of PKC, NADPH oxidase, and NOS. DNA damage was measured by the comet assay and the micronucleus frequency test in LLC-PK1 and MDCK cells, incubated in the absence (C) and presence of 10 nM aldosterone for 4 h. Results are shown as the percentage of DNA in the tail or as micronuclei-containing cells (MN) per 1000 binucleated cells (BN). Aldosterone-treated cells were simultaneously incubated without (Ald) or with (A, B) the calcium chelator BAPTA-AM (Bapta; 10 μM), 5 μM 2-APB (APB; inhibitor of store-operated calcium channels and IP_3 receptors), or 0.2 μM thapsigargin (TG; sarcoplasmic/endoplasmic reticulum calcium inhibitor) or in calcium-free medium (Ca−), or with (C, D) 1 μM DPI (DPI), 50 μM apocynin (Apo), or 1 μM VAS2870 (VAS) (NADPH oxidase inhibitors) or 1 μM Ro (Ro; PKC inhibitor), or with (E, F) 50 μM L-NAME (LN; NOS inhibitor) or 10 μM W-7 (W7; calmodulin inhibitor). (G) Oxidative DNA damage measured by the FPG-modified comet assay in LLC-PK1 and MDCK cells after 4 h treatment and incubated in the absence (C) and presence of 10 nM aldosterone. Cells were simultaneously incubated with 50 μM LN or 10 μM W7. Depicted is the mean of the difference (Δ) in the percentage of DNA in the tail between nuclei treated and untreated with the FPG enzyme. Results are shown as means ± SEM of at least three independent experiments. $^{*}p \leq 0.05$, significantly different from the control, and $^{\#}p \leq 0.05$, significantly different from the aldosterone-treated group.

DPI, apocynin, and VAS2870 and the PKC inhibitor Ro (Fig. 5A). Supporting the involvement of calmodulin/NOS, and therefore of RNS, in aldosterone-induced NF-κB activation, the NOS inhibitor L-NAME and the calmodulin inhibitor W-7 inhibited the increase in NF-κB–DNA binding (Fig. 5B). As expected, given that NADPH oxidase and NOS were activated by aldosterone through an increase in cellular calcium levels, BAPTA-AM completely prevented aldosterone-induced NF-κB activation (Fig. 5B).

Aldosterone induces DNA damage via the calcium-mediated activation of PKC, NADPH oxidase, and NOS

Aldosterone-associated DNA damage was analyzed using two genotoxicity tests: the comet assay and the micronucleus frequency test. To follow the hypothesis that aldosterone-induced DNA damage is mediated by a rise in intracellular calcium, the effects of various calcium inhibitors and of calcium-free medium were next characterized.

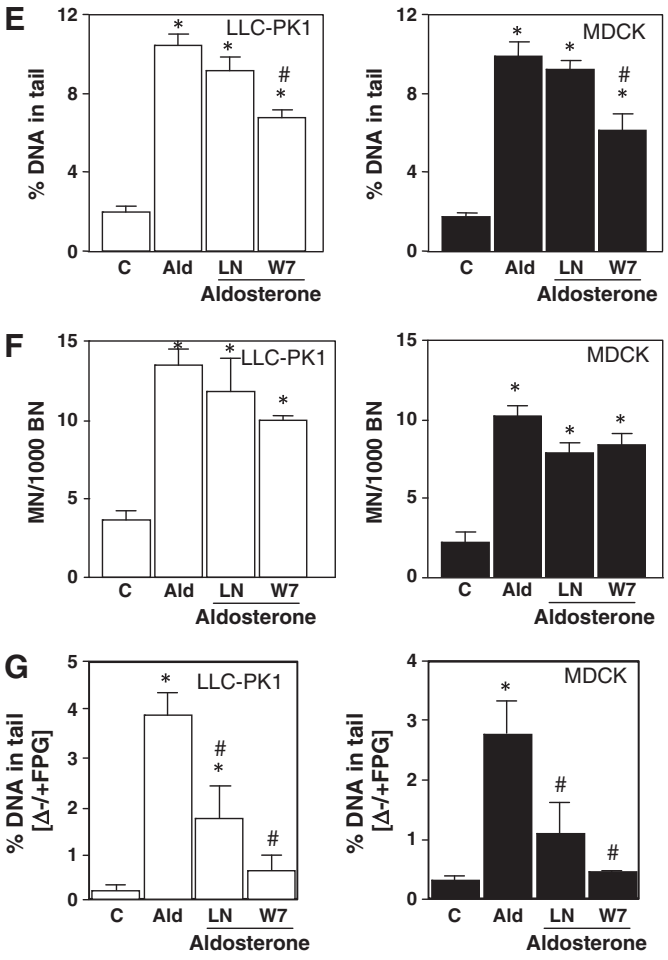

Fig. 6 (*continued*).

Aldosterone-triggered DNA damage was inhibited when cells were incubated in a calcium-free medium or in the presence of calcium chelators, BAPTA-AM, 2-APB (an inhibitor of store-operated calcium channels and IP_3 receptors), and thapsigargin (sarcoplasmic/endoplasmic reticulum calcium inhibitor), as evidenced by both the comet assay (Fig. 6A) and the micronucleus frequency test (Fig. 6B) in LLC-PK1 and MDCK cells.

DNA damage was also diminished by the PKC inhibitor Ro, as well as by the NADPH oxidase inhibitors DPI, apocynin, and VAS2870 (Figs. 6C and D) in both cell lines. The NOS inhibitors L-NAME and W-7 only partially decreased DNA damage in the comet assay (Fig. 6E) and in the micronucleus test (Fig. 6F) in LLC-PK1 and MDCK cells. Given that no clear involvement of NOS in the aldosterone-mediated DNA damage was observed using the normal alkaline comet assay, which detects strand breaks and abasic sites, the comet assay was performed with an additional incubation in the presence of the DNA repair enzyme FPG. This allows the quantification of the oxidative base modification 8-oxodG. The FPG enzyme incises the DNA at the site of the lesion, thereby generating additional strand breaks. Treatment with aldosterone significantly increased the occurrence of FPG-sensitive sites in LLC-PK1 and MDCK cells, which was inhibited by the NOS inhibitors L-NAME and W-7 in both cell lines (Fig. 6G), indicating that NOS is involved specifically in aldosterone-induced formation of 8-oxodG.

Discussion

We previously demonstrated that aldosterone is genotoxic in kidney tubule cells and causes the activation of NF-κB, with evidence that an increase in cellular oxidants in part triggers those effects [16,31]. Both DNA damage and chronic NF-κB activation can lead to oncogenesis. Understanding the mechanism underlying aldosterone-induced oxidant production is essential in the development of therapies that could prevent the adverse effects of chronic aldosteronism, particularly the potential increase in kidney cancer risk.

We observed that aldosterone causes an increase in ROS and RNS in LLC-PK1 and MDCK cells, derived from different parts of kidney tubules. Aldosterone-induced increase in ROS occurs as a consequence of a calcium-mediated activation of NADPH oxidase. In fact, previous evidence showed that treatment of rats with aldosterone causes kidney oxidative stress and the activation of NADPH oxidase [22]. It is currently known that at least five different isoforms of the NADPH oxidase subunit NOX (1–5) and two homologous oxidases (Duox1, Duox2) exist in eukaryotic cells [38]. From them, the one present in macrophages (NOX2) is the most extensively characterized. NOX's 1, 2, and 4 have been identified in the kidney, whereas NOX4 is the predominant isoform expressed in the tubular epithelium [19]. In a cell line model of renal proximal tubule cells (human hRPT) the presence of NOX2 and NOX4 was recently described [17]. NADPH oxidase can be activated by calcium either directly or indirectly. NOX5 is the only isoform that can be directly activated by calcium. The other isoforms can be activated indirectly, via a calcium-mediated activation of PKC that subsequently activates NADPH oxidase [39,40]. The finding that Ro inhibited the increase in ROS caused by aldosterone indicates that the isoforms activated in LLC-PK1 and MDCK cells are regulated by calcium via PKC.

Aldosterone also induced an increase in LLC-PK1 and MDCK cell RNS levels. This increase occurs as a consequence of the activation of NOS, the enzyme that generates NO from L-arginine in the presence

of NADPH and oxygen. NOS is considered to have protective effects on the kidney. Mice genetically deficient in endothelial NOS are characterized by kidney damage that includes glomerular hypoplasia and death of tubular cells [41]. Although NOS activation and NO production are important in vasorelaxation, which also involves the kidney vasculature, excess NO can lead to damage of cellular components and ultimately to cell death. In this regard, iNOS activation is involved in the proximal tubular damage in sepsis, and iNOS inhibitors are being studied as a protective therapy for this injury [42]. We observed that the activation of NOS and the associated production of RNS by aldosterone have significant functional consequences in LLC-PK1 and MDCK cells. In this regard, the activation of NF-κB is central to inflammation and, in association with DNA damage, could be a major player in carcinogenesis.

The activation of NADPH oxidase and NOS by aldosterone occurs as a consequence of an increase in cellular calcium. An increase in calcium by aldosterone was previously reported in various cell types [43–45]. We used various inhibitors and conditions to evaluate the source of this calcium increase. The marked decrease in calcium level observed in aldosterone-treated cells incubated in calcium-free medium indicates that aldosterone causes cellular calcium influx. Significantly, the calcium channel blocker dihydropyridine protects the kidney from aldosterone-induced NADPH oxidase activation and injury in rats [23]. In spontaneously hypertensive rats, benidipine, an inhibitor of L-type and T-type calcium channels, protected the kidney from damage through the inhibition of NADPH oxidase [46]. On the other hand, the inhibitory effect of thapsigargin indicates that calcium is also mobilized from thapsigargin-sensitive stores. An intracellular source of the increased cytosolic calcium in LLC-PK1 and MDCK cells exposed to aldosterone is also supported by the inhibitory action of the calcium chelator BAPTA-AM and 2-APB, a blocker of IP_3 receptors [34] and of store-operated calcium channels [47]. Over the range 1–100 μM, 2-APB inhibited calcium signals by preventing its release from intracellular stores and subsequent calcium entry [33]. The concentration of 2-APB used in this study supports this mechanism for the action of aldosterone on calcium metabolism in kidney tubule cells. Therefore, aldosterone signaling seems to involve a combination of release of calcium from intracellular stores and influx of calcium across the plasma membrane.

Aldosterone-induced ROS and RNS increases in kidney tubule cells are mediated by the mineralocorticoid receptor. This was evidenced by their preventability with the highly specific mineralocorticoid receptor blocker eplerenone [48,49] and the lack of effect of the glucocorticoid receptor inhibitor mifepristone. In agreement with Grossmann et al. [50], aldosterone-mediated calcium increase in MDCK cells was not inhibitable by eplerenone. This was the only difference in aldosterone signaling found in the course of this work between LLC-PK1 and MDCK cells. Although nongenomic effects of aldosterone are well established, the receptor-mediated mechanisms responsible remain unclear [14]. There is evidence for rapid effects of aldosterone dependent on and independent of the classical mineralocorticoid receptor, possibly mediated through a novel but yet unknown receptor [11]. The results suggest a mineralocorticoid receptor-dependent calcium signal in LLC-PK1 cells and mineralocorticoid receptor-independent calcium signal in MDCK cells. This is the first evidence for the existence of two different receptors mediating aldosterone signaling in MDCK cells.

Aldosterone-induced DNA damage was dependent on the increase in intracellular calcium. It was previously described that increased cytosolic calcium itself could be responsible for the formation of DNA strand breaks [51]. Disruption of the calcium homeostasis is strongly correlated with micronucleus formation and the induction of mitotic disturbances [52,53]. In the case of aldosterone-induced DNA damage the most important consequence of calcium increase is the activation of NADPH oxidase and the increase in $O_2^{\bullet-}$ [16,31]. The NADPH oxidase inhibitors DPI, apocynin, and VAS2870 significantly reduced DNA damage in both cell lines. Over 100 oxidative DNA modifications were identified [54], among them 8-oxodG, which is formed by hydroxyl radicals attacking guanine residues. We recently reported that 8-oxodG is increased in aldosterone-treated cells as well as in animals with mineralocorticoid-dependent hypertension [55]. Furthermore, the characterization of the DNA bases that are affected by aldosterone showed that NOS activation specifically results in an increase in the oxidized base 8-oxodG as shown in the FPG-comet assay. Huang et al. [56] observed that NO causes nitrosative and oxidative stress, leading to the accumulation of 8-nitroguanine and 8-oxodG. Furthermore, NO also inhibits the human enzyme that repairs 8-oxodG, 8-oxodG DNA glycosylase [57]. This enzyme contains critical thiol moieties and thus is potentially susceptible to inactivation by nitrosylation reactions of NO. Thus, the inhibition of DNA repair processes and potentiation of oxidative DNA damage by NO would be expected to increase the rate of mutagenic DNA lesions [58]. In agreement with our findings, this observation suggests an integral role for NO in promoting oxidative DNA damage.

In summary, our results indicate that aldosterone increases kidney tubule cell oxidant levels mainly through its interaction with the mineralocorticoid receptor. This triggers an increase in cellular calcium that can originate from both mobilization of intracellular stores and calcium influx. The increased cellular calcium leads to a PKC-mediated NADPH oxidase activation and to a calmodulin-mediated NOS activation, which is the cause of the initial increase in tubule cell oxidants. High levels of oxidants trigger two events that can participate in carcinogenesis, DNA damage and NF-κB activation. Therapies targeting calcium, NOS, and NOX could prevent the adverse effects of aldosterone on kidney function and also its possible oncogenic action.

Acknowledgments

This work was supported by grants from the University of California at Davis (USA) and by Deutsche Forschungsgemeinschaft Grant Schu 2367/1-1 (to N.S. and H.S.) (Germany). N.Q. was supported by a fellowship from the DAAD (Germany).

References

[1] Friis, S.; Sorensen, H. T.; Mellemkjaer, L.; McLaughlin, J. K.; Nielsen, G. L.; Blot, W. J.; Olsen, J. H. Angiotensin-converting enzyme inhibitors and the risk of cancer: a population-based cohort study in Denmark. *Cancer* **92:**2462–2470; 2001.

[2] Moore, L. E.; Wilson, R. T.; Campleman, S. L. Lifestyle factors, exposures, genetic susceptibility, and renal cell cancer risk: a review. *Cancer Invest.* **23:**240–255; 2005.

[3] Grossman, E.; Messerli, F. H.; Boyko, V.; Goldbourt, U. Is there an association between hypertension and cancer mortality? *Am. J. Med.* **112:**479–486; 2002.

[4] Corrao, G.; Scotti, L.; Bagnardi, V.; Sega, R. Hypertension, antihypertensive therapy and renal-cell cancer: a meta-analysis. *Curr. Drug Safe* **2:**125–133; 2007.

[5] Funder, J.; New, M. I. Low renin hypertension (LRH): shades of John Laragh. *Trends Endocrinol. Metab.* **19:**83; 2008.

[6] Rossi, G. P.; Bernini, G.; Caliumi, C.; Desideri, G.; Fabris, B.; Ferri, C.; Ganzaroli, C.; Giacchetti, G.; Letizia, C.; Maccario, M.; Mallamaci, F.; Mannelli, M.; Mattarello, M. J.; Moretti, A.; Palumbo, G.; Parenti, G.; Porteri, E.; Semplicini, A.; Rizzoni, D.; Rossi, E.; Boscaro, M.; Pessina, A. C.; Mantero, F. A prospective study of the prevalence of primary aldosteronism in 1,125 hypertensive patients. *J. Am. Coll. Cardiol.* **48:**2293–2300; 2006.

[7] Gordon, R. D.; Ziesak, M. D.; Tunny, T. J.; Stowasser, M.; Klemm, S. A. Evidence that primary aldosteronism may not be uncommon: 12% incidence among antihypertensive drug trial volunteers. *Clin. Exp. Pharmacol. Physiol.* **20:**296–298; 1993.

[8] Calhoun, D. A.; Jones, D.; Textor, S.; Goff, D. C.; Murphy, T. P.; Toto, R. D.; White, A.; Cushman, W. C.; White, W.; Sica, D.; Ferdinand, K.; Giles, T. D.; Falkner, B.; Carey, R. M. Resistant hypertension: diagnosis, evaluation, and treatment. A scientific statement from the American Heart Association Professional Education Committee of the Council for High Blood Pressure Research. *Circulation* **117:**e510–526; 2008.

[9] Marney, A. M.; Brown, N. J. Aldosterone and end-organ damage. *Clin. Sci. (London)* **113:**267–278; 2007.

[10] Connell, J. M.; Davies, E. The new biology of aldosterone. *J. Endocrinol.* **186:**1–20; 2005.

[11] Good, D. W. Nongenomic actions of aldosterone on the renal tubule. *Hypertension* **49:**728–739; 2007.

[12] Boldyreff, B.; Wehling, M. Rapid aldosterone actions: from the membrane to signaling cascades to gene transcription and physiological effects. *J. Steroid Biochem. Mol. Biol.* **85:**375–381; 2003.

[13] Skott, O.; Uhrenholt, T. R.; Schjerning, J.; Hansen, P. B.; Rasmussen, L. E.; Jensen, B. L. Rapid actions of aldosterone in vascular health and disease—friend or foe? *Pharmacol. Ther.* **111:**495–507; 2006.

[14] Harvey, B. J.; Alzamora, R.; Stubbs, A. K.; Irnaten, M.; McEneaney, V.; Thomas, W. Rapid responses to aldosterone in the kidney and colon. *J. Steroid Biochem. Mol. Biol.* **108:**310–317; 2008.

[15] Hayashi, H.; Kobara, M.; Abe, M.; Tanaka, N.; Gouda, E.; Toba, H.; Yamada, H.; Tatsumi, T.; Nakata, T.; Matsubara, H. Aldosterone nongenomically produces NADPH oxidase-dependent reactive oxygen species and induces myocyte apoptosis. *Hypertens. Res.* **31:**363–375; 2008.

[16] Queisser, N.; Oteiza, P. I.; Stopper, H.; Oli, R. G.; Schupp, N. Aldosterone induces oxidative stress, oxidative DNA damage and NF-kappaB-activation in kidney tubule cells. *Mol. Carcinog.* **50:**123–135; 2011.

[17] Han, W.; Li, H.; Villar, V. A.; Pascua, A. M.; Dajani, M. I.; Wang, X.; Natarajan, A.; Quinn, M. T.; Felder, R. A.; Jose, P. A.; Yu, P. Lipid rafts keep NADPH oxidase in the inactive state in human renal proximal tubule cells. *Hypertension* **51:** 481–487; 2008.

[18] Gill, P. S.; Wilcox, C. S. NADPH oxidases in the kidney. *Antioxid. Redox Signal.* **8:** 1597–1607; 2006.

[19] Schreck, C.; O'Connor, P. M. NAD(P)H oxidase and renal epithelial ion transport. *Am. J. Physiol. Regul. Integr. Comp. Physiol.* **300:**R1023–R1029; 2011.

[20] Santolini, J. The molecular mechanism of mammalian NO-synthases: a story of electrons and protons. *J. Inorg. Biochem.* **105:**127–141; 2011.

[21] Hill, B. G.; Dranka, B. P.; Bailey, S. M.; Lancaster Jr., J. R.; Darley-Usmar, V. M. What part of NO don't you understand? Some answers to the cardinal questions in nitric oxide biology. *J. Biol. Chem.* **285:**19699–19704; 2010.

[22] Trebak, M.; Ginnan, R.; Singer, H. A.; Jourd'heuil, D. Interplay between calcium and reactive oxygen/nitrogen species: an essential paradigm for vascular smooth muscle signaling. *Antioxid. Redox Signal.* **12:**657–674; 2010.

[23] Fan, Y. Y.; Kohno, M.; Nakano, D.; Hitomi, H.; Nagai, Y.; Fujisawa, Y.; Lu, X. M.; Fu, H.; Du, J.; Ohmori, K.; Hosomi, N.; Kimura, S.; Kiyomoto, H.; Nishiyama, A. Inhibitory effects of a dihydropyridine calcium channel blocker on renal injury in aldosterone-infused rats. *J. Hypertens.* **27:**1855–1862; 2009.

[24] Rasband, W. S. Image J software program. U.S. National Institutes of Health, Bethesda (MD; 1997–2008.

[25] Mackenzie, G. G.; Zago, M. P.; Keen, C. L.; Oteiza, P. I. Low intracellular zinc impairs the translocation of activated NF-kappa B to the nuclei in human neuroblastoma IMR-32 cells. *J. Biol. Chem.* **277:**34610–34617; 2002.

[26] Bradford, M. M. A rapid and sensitive method for the quantitation of microgram quantities of protein utilizing the principle of protein–dye binding. *Anal. Biochem.* **72:**248–254; 1976.

[27] Schupp, N.; Schmid, U.; Rutkowski, P.; Lakner, U.; Kanase, N.; Heidland, A.; Stopper, H. Angiotensin II-induced genomic damage in renal cells can be prevented by angiotensin II type 1 receptor blockage or radical scavenging. *Am. J. Physiol. Ren. Physiol.* **292:**F1427–1434; 2007.

[28] Schmid, U.; Stopper, H.; Schweda, F.; Queisser, N.; Schupp, N. Angiotensin II induces DNA damage in the kidney. *Cancer Res.* **68:**9239–9246; 2008.

[29] Leckie, C.; Chapman, K. E.; Edwards, C. R.; Seckl, J. R. LLC-PK1 cells model 11 beta-hydroxysteroid dehydrogenase type 2 regulation of glucocorticoid access to renal mineralocorticoid receptors. *Endocrinology* **136:**5561–5569; 1995.

[30] Simmons, N. L. Cultured monolayers of MDCK cells: a novel model system for the study of epithelial development and function. *Gen. Pharmacol.* **13:**287–291; 1982.

[31] Schupp, N.; Queisser, N.; Wolf, M.; Kolkhof, P.; Barfacker, L.; Schafer, S.; Heidland, A.; Stopper, H. Aldosterone causes DNA strand breaks and chromosomal damage in renal cells, which are prevented by mineralocorticoid receptor antagonists. *Horm. Metab. Res.* **42:**458–465; 2010.

[32] Crow, J. P. Dichlorodihydrofluorescein and dihydrorhodamine 123 are sensitive indicators of peroxynitrite in vitro: implications for intracellular measurement of reactive nitrogen and oxygen species. *Nitric Oxide* **1:**145–157; 1997.

[33] Bootman, M. D.; Collins, T. J.; Mackenzie, L.; Roderick, H. L.; Berridge, M. J.; Peppiatt, C. M. 2-Aminoethoxydiphenyl borate (2-APB) is a reliable blocker of store-operated Ca^{2+} entry but an inconsistent inhibitor of InsP3-induced Ca^{2+} release. *FASEB J.* **16:** 1145–1150; 2002.

[34] Maruyama, T.; Kanaji, T.; Nakade, S.; Kanno, T.; Mikoshiba, K. 2APB, 2-aminoethoxydiphenyl borate, a membrane-penetrable modulator of Ins(1,4,5) P3-induced Ca^{2+} release. *J. Biochem.* **122:**498–505; 1997.

[35] Heumuller, S.; Wind, S.; Barbosa-Sicard, E.; Schmidt, H. H.; Busse, R.; Schroder, K.; Brandes, R. P. Apocynin is not an inhibitor of vascular NADPH oxidases but an antioxidant. *Hypertension* **51:**211–217; 2008.

[36] ten Freyhaus, H.; Huntgeburth, M.; Wingler, K.; Schnitker, J.; Baumer, A. T.; Vantler, M.; Bekhite, M. M.; Wartenberg, M.; Sauer, H.; Rosenkranz, S. Novel Nox inhibitor VAS2870 attenuates PDGF-dependent smooth muscle cell chemotaxis, but not proliferation. *Cardiovasc. Res.* **71:**331–341; 2006.

[37] Lobysheva, I.; Rath, G.; Sekkali, B.; Bouzin, C.; Feron, O.; Gallez, B.; Dessy, C.; Balligand, J. L. Moderate caveolin-1 downregulation prevents NADPH oxidase-dependent endothelial nitric oxide synthase uncoupling by angiotensin II in endothelial cells. *Arterioscler. Thromb. Vasc. Biol.* **31:**2098–2105; 2011.

[38] Lambeth, J. D. NOX enzymes and the biology of reactive oxygen. *Nat. Rev. Immunol.* **4:**181–189; 2004.

[39] Noh, K. M.; Koh, J. Y. Induction and activation by zinc of NADPH oxidase in cultured cortical neurons and astrocytes. *J. Neurosci.* **20:**RC111; 2000.

[40] Siow, Y. L.; Au-Yeung, K. K.; Woo, C. W.; O, K. Homocysteine stimulates phosphorylation of NADPH oxidase p47phox and p67phox subunits in monocytes via protein kinase Cbeta activation. *Biochem. J.* **398:**73–82; 2006.

[41] Forbes, M. S.; Thornhill, B. A.; Park, M. H.; Chevalier, R. L. Lack of endothelial nitric-oxide synthase leads to progressive focal renal injury. *Am. J. Pathol.* **170:** 87–99; 2007.

[42] Heemskerk, S.; Masereeuw, R.; Russel, F. G.; Pickkers, P. Selective iNOS inhibition for the treatment of sepsis-induced acute kidney injury. *Nat. Rev. Nephrol.* **5:** 629–640; 2009.

[43] Losel, R. M.; Feuring, M.; Falkenstein, E.; Wehling, M. Nongenomic effects of aldosterone: cellular aspects and clinical implications. *Steroids* **67:**493–498; 2002.

[44] Gekle, M.; Freudinger, R.; Mildenberger, S.; Silbernagl, S. Aldosterone interaction with epidermal growth factor receptor signaling in MDCK cells. *Am. J. Physiol. Renal Physiol.* **282:**F669–679; 2002.

[45] Harvey, B. J.; Higgins, M. Nongenomic effects of aldosterone on Ca^{2+} in M-1 cortical collecting duct cells. *Kidney Int.* **57:**1395–1403; 2000.

[46] Yamamoto, E.; Kataoka, K.; Dong, Y. F.; Nakamura, T.; Fukuda, M.; Nako, H.; Ogawa, H.; Kim-Mitsuyama, S. Benidipine, a dihydropyridine L-type/T-type calcium channel blocker, affords additive benefits for prevention of cardiorenal injury in hypertensive rats. *J. Hypertens.* **28:**1321–1329; 2010.

[47] Prakriya, M.; Lewis, R. S. Potentiation and inhibition of Ca^{2+} release-activated Ca^{2+} channels by 2-aminoethyldiphenyl borate (2-APB) occurs independently of IP (3) receptors. *J. Physiol.* **536:**3–19; 2001.

[48] Rogerson, F. M.; Yao, Y.; Smith, B. J.; Fuller, P. J. Differences in the determinants of eplerenone, spironolactone and aldosterone binding to the mineralocorticoid receptor. *Clin. Exp. Pharmacol. Physiol.* **31:**704–709; 2004.

[49] Muldowney III, J. A.; Schoenhard, J. A.; Benge, C. D. The clinical pharmacology of eplerenone. *Expert Opin. Drug Metab. Toxicol.* **5:**425–432; 2009.

[50] Grossmann, C.; Benesic, A.; Krug, A. W.; Freudinger, R.; Mildenberger, S.; Gassner, B.; Gekle, M. Human mineralocorticoid receptor expression renders cells responsive for nongenotropic aldosterone actions. *Mol. Endocrinol.* **19:**1697–1710; 2005.

[51] Florea, A. M.; Yamoah, E. N.; Dopp, E. Intracellular calcium disturbances induced by arsenic and its methylated derivatives in relation to genomic damage and apoptosis induction. *Environ. Health Perspect.* **113:**659–664; 2005.

[52] Dopp, E.; Muller, J.; Hahnel, C.; Schiffmann, D. Induction of genotoxic effects and modulation of the intracellular calcium level in Syrian hamster embryo (SHE) fibroblasts caused by ochratoxin A. *Food Chem. Toxicol.* **37:**713–721; 1999.

[53] Xu, N.; Luo, K. Q.; Chang, D. C. Ca^{2+} signal blockers can inhibit M/A transition in mammalian cells by interfering with the spindle checkpoint. *Biochem. Biophys. Res. Commun.* **306:**737–745; 2003.

[54] Lu, A. L.; Li, X.; Gu, Y.; Wright, P. M.; Chang, D. Y. Repair of oxidative DNA damage: mechanisms and functions. *Cell Biochem. Biophys.* **35:**141–170; 2001.

[55] Schupp, N.; Kolkhof, P.; Queisser, N.; Gartner, S.; Schmid, U.; Kretschmer, A.; Hartmann, E.; Oli, R. G.; Schafer, S.; Stopper, H. Mineralocorticoid receptor-mediated DNA damage in kidneys of DOCA-salt hypertensive rats. *FASEB J.* **25:**968–978; 2011.

[56] Huang, Y. J.; Zhang, B. B.; Ma, N.; Murata, M.; Tang, A. Z.; Huang, G. W. Nitrative and oxidative DNA damage as potential survival biomarkers for nasopharyngeal carcinoma. *Med. Oncol.* **28:**377–384; 2011.

[57] Jaiswal, M.; LaRusso, N. F.; Nishioka, N.; Nakabeppu, Y.; Gores, G. J. Human Ogg1, a protein involved in the repair of 8-oxoguanine, is inhibited by nitric oxide. *Cancer Res.* **61:**6388–6393; 2001.

[58] Jaiswal, M.; LaRusso, N. F.; Shapiro, R. A.; Billiar, T. R.; Gores, G. J. Nitric oxide-mediated inhibition of DNA repair potentiates oxidative DNA damage in cholangiocytes. *Gastroenterology* **120:**190–199; 2001.